Pre-kinking analysis of a cracked piezoelectric strip under impact loadings

Zengtao Chen[1,*], **Keqiang Hu**[1]

[1] Department of Mechanical Engineering, University of New Brunswick, Fredericton NB E3B 5A3, Canada
* Corresponding author: ztchen@unb.ca

Abstract An impermeable crack in a piezoelectric strip at arbitrary position under in-plane mechanical and electric impact loadings is considered. Due to the asymmetry of the geometry, this crack problem is a mixed-mode one. Fourier and Laplace transforms are applied to reduce the mixed boundary value problem of the crack to a system of singular integral equations. The asymptotic fields near the crack tip are obtained in explicit form and hoop and shear stress intensity factors are defined. Laplace inversion transforms are applied to get the dynamic hoop stress intensity factors. The crack kinking phenomena is investigated by applying the criterion of maximum hoop stress intensity factors. Numerical results show that the geometry of the cracked strip and the electric loadings have effects on the singular field distributions around the crack tip, and the hoop stress intensity factors are influenced by the material parameters, the electric loading and the geometric size ratios.

Keywords Mixed-mode crack, Piezoelectric Strip, Singular integral equations, Crack kinking; Hoop stress intensity factor

1. Introduction

Piezoelectric materials can be made into various functional devices, such as sensors and actuators, which are widely used in modern industrial fields. Due to the brittleness and low fracture toughness of piezoelectric materials, dynamic fracture analysis of piezoelectric materials has drawn considerable attentions. Dynamic anti-plane crack propagation in piezoelectric materials has been studied by Li and Mataga [1, 2]. Shindo et al. [3] obtained dynamic stress intensity factors of a cracked piezoelectric medium in a uniform dielectric field. The problem of a Griffith crack moving along the interface of two dissimilar piezoelectric materials was solved by Chen et al. [4] using the integral transform technique and it is shown that the stress and electric displacement are dependent on the speed of the crack and the material coefficients. Chen and Yu [5] investigated a semi-infinite crack in a piezoelectric medium subjected to antiplane impact loading. Mode-I transient response of a piezoelectric strip containing a center-situated crack under in-plane mechanical and electric impacts was investigated by Wang and Yu [6], and it was found that the intrinsic mechanical-electrical coupling plays a significant role in the dynamic fracture response of in-plane problems.

Crack kinking is an important phenomenon in the fracture of piezoelectric materials in response to electro-mechanical loading. Zhu and Yang [7] modeled the crack kinking in a piezoelectric solid by continuous distribution of edge dislocations and electric dipoles, and the solution was formulated via the Stroh formalism. The mixed-mode crack initiation in piezoelectric strip was studied by Wang and Noda [8] using the method of Fourier transform and singular integral equations. Hu and Zhong [9] considered a moving mode-III crack in a functionally graded piezoelectric strip. They found that the gradient of the material properties can affect the magnitudes of the stress intensity factors, and a high crack moving velocity can change the propagation orientation of the crack.

In this paper, the mixed-mode crack in a piezoelectric strip under in-plane electrical and mechanical impact loadings is studied. Fourier transform is employed to reduce the mixed boundary

value problem of the crack to solving a system of singular integral equations. The asymptotic fields near the crack tip are obtained in an explicit form and the hoop and shear stress intensity factors are then determined. The crack kinking phenomenon is investigated by applying the maximum hoop stress intensity factor criterion. The coupled electro-mechanical effects on the crack-tip fields are investigated and the influence of the geometric feature of the strip on the crack kinking is discussed.

2. Problem statement and method of solution

Consider a transversely isotropic, linear piezoelectric material and denote the rectangular coordinates of a point by (x, y, z). The constitutive equations can be written as

$$\begin{Bmatrix}\sigma_{xx}\\ \sigma_{zz}\\ \sigma_{xz}\end{Bmatrix}=\begin{bmatrix}C_{11} & C_{13} & 0\\ C_{13} & C_{33} & 0\\ 0 & 0 & C_{44}\end{bmatrix}\begin{Bmatrix}\partial u_x/\partial x\\ \partial u_z/\partial z\\ \partial u_x/\partial z+\partial u_z/\partial x\end{Bmatrix}+\begin{bmatrix}0 & e_{31}\\ 0 & e_{33}\\ e_{15} & 0\end{bmatrix}\begin{Bmatrix}\partial\phi/\partial x\\ \partial\phi/\partial z\end{Bmatrix}$$
$$\begin{Bmatrix}D_x\\ D_z\end{Bmatrix}=\begin{bmatrix}0 & 0 & e_{15}\\ e_{31} & e_{33} & 0\end{bmatrix}\begin{Bmatrix}\partial u_x/\partial x\\ \partial u_z/\partial z\\ \partial u_x/\partial z+\partial u_z/\partial x\end{Bmatrix}-\begin{bmatrix}\lambda_{11} & 0\\ 0 & \lambda_{33}\end{bmatrix}\begin{Bmatrix}\partial\phi/\partial x\\ \partial\phi/\partial z\end{Bmatrix} \quad (1)$$

where u_x, u_z are components of the displacement vector and ϕ is the electric potential, $C_{11}, C_{13}, C_{33}, C_{44}$ are elastic constants, e_{15}, e_{31} are piezoelectric constants, and $\lambda_{11}, \lambda_{33}$ are dielectric permittivities, σ_{ij} and D_i ($i, j = x, z$) are components of stress and electric displacement, respectively.

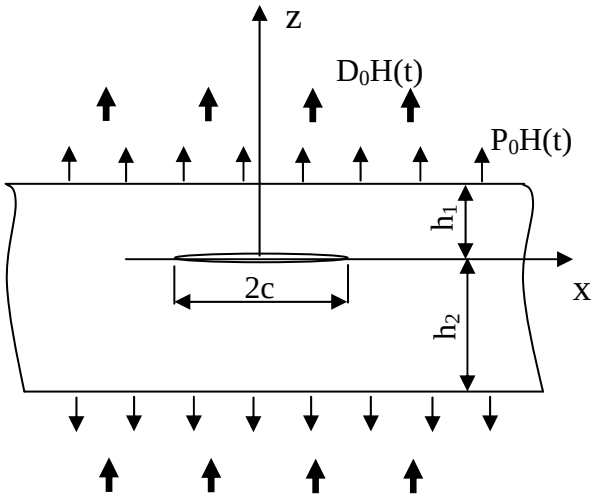

Figure 1. A cracked piezoelectric strip under in-plane mechanical and electric impact loadings

Studied in this paper is a Griffith crack of length $2c$ in a piezoelectric strip of width $h_1 + h_2$, with the poling direction perpendicular to the crack plane, as shown in Fig. 1. Uniform impact

normal stress $P_0\mathrm{H(t)}$ and impact electric displacement $D_0\mathrm{H(t)}$ are applied on the edges of the strip, where H(t) is the Heaviside step function. As shown in Fig. 1, symmetry conditions are used to allow for consideration of only the region ($x \geq 0,\ -h_2 \leq z \leq h_1$). In this paper the impermeable electric boundary condition on the crack faces is employed.

Application of Laplace transform leads to the governing equations in the Laplace domain as follows:

$$\begin{aligned} &C_{11}u^*_{x,xx} + C_{44}u^*_{x,zz} + (C_{13}+C_{44})u^*_{z,xz} + (e_{31}+e_{15})\phi^*_{,xz} = \rho p^2 u^*_x \\ &(C_{13}+C_{44})u^*_{x,xz} + C_{44}u^*_{z,xx} + C_{33}u^*_{z,zz} + e_{15}\phi^*_{,xx} + e_{33}\phi^*_{,zz} = \rho p^2 u^*_z \\ &(e_{31}+e_{15})u^*_{x,xz} + e_{15}u^*_{z,xx} + e_{33}u^*_{z,zz} - \lambda_{11}\phi^*_{,xx} - \lambda_{33}\phi^*_{,zz} = 0 \end{aligned} \tag{2}$$

where p is the Laplace transform parameter and the superscript * denotes the quantities in the Laplace transform domain.

The corresponding boundary conditions and continuity conditions in the Laplace domain are:

$$\sigma^*_{zz}(x,h_1,p) = \sigma^*_{zz}(x,-h_2,p) = P_0/p,\ \ \sigma^*_{xz}(x,h_1,p) = \sigma^*_{xz}(x,-h_2,p) = 0 \qquad (x \geq 0) \tag{3}$$

$$D^*_z(x,h_1,p) = D^*_z(x,-h_2,p) = D_0/p$$

$$\sigma^*_{zz}(x,0^+,p) = \sigma^*_{zz}(x,0^-,p),\ \ \sigma^*_{xz}(x,0^+,p) = \sigma^*_{xz}(x,0^-,p) \qquad (x \geq 0) \tag{4}$$

$$D^*_z(x,0^+,p) = D^*_z(x,0^-,p)$$

$$\sigma^*_{zz}(x,0,p) = 0,\ \ \sigma^*_{xz}(x,0,p) = 0,\ \ D^*_z(x,0,p) = 0 \qquad (0 \leq x < c) \tag{5}$$

$$u^*_z(x,0^+,p) = u^*_z(x,0^-,p),\ \ u^*_x(x,0^+,p) = u^*_x(x,0^-,p) \qquad (x \geq c) \tag{6}$$

$$\phi^*(x,0^+,p) = \phi^*(x,0^-,p)$$

Fourier transform is applied to Eq. (2) to obtain the solutions as

$$u^{*(n)}_x(x,z,p) = -\sum_{j=1}^{3}\int_0^\infty a_j\gamma_j\left[A^{(n)}_j(\xi,p)\sinh(\gamma_j\xi z) + B^{(n)}_j(\xi,p)\cosh(\gamma_j\xi z)\right]\sin(\xi x)d\xi \tag{7}$$

$$u^{*(n)}_z(x,z,p) = \sum_{j=1}^{3}\int_0^\infty \left[A^{(n)}_j(\xi,p)\cosh(\gamma_j\xi z) + B^{(n)}_j(\xi,p)\sinh(\gamma_j\xi z)\right]\cos(\xi x)d\xi + T_1 z/p \tag{8}$$

$$\phi^{*(n)}(x,z,p) = -\sum_{j=1}^{3}\int_0^\infty b_j\left[A^{(n)}_j(\xi,p)\cosh(\gamma_j\xi z) + B^{(n)}_j(\xi,p)\sinh(\gamma_j\xi z)\right]\cos(\xi x)d\xi + T_2 z/p \tag{9}$$

where T_j $(j=1,2)$ are constants and a_j, b_j $(j=1,2,3)$ are known functions defined in Appendix A, the superscripts $(n)=(1),\ (2)$ denote the fields quantities in the upper ($0 \leq y \leq h_1$) and lower ($-h_2 \leq y \leq 0$) parts of the piezoelectric strip, respectively, and $A^{(n)}_j(\xi,p)$, $B^{(n)}_j(\xi,p)$, $(n=1,2;\ j=1,2,3)$ are unknowns to be determined; γ_j ($j=1-3$) are the roots of the following characteristic equation:

$$\begin{vmatrix} C_{11}+\rho p^2/\xi^2-C_{44}\gamma^2 & (C_{13}+C_{44})\gamma & (e_{31}+e_{15})\gamma \\ (C_{13}+C_{44})\gamma & C_{33}\gamma^2-\rho p^2/\xi^2-C_{44} & e_{33}\gamma^2-e_{15} \\ (e_{31}+e_{15})\gamma & e_{33}\gamma^2-e_{15} & \lambda_{11}-\lambda_{33}\gamma^2 \end{vmatrix}=0 \tag{10}$$

Note that the sixth-order characteristic equation (10) has six roots which occur in pairs with the same magnitude but opposite signs, and for complex roots, they always appear in conjugate pairs. In Eqs. (7-9), the roots γ_j ($j=1-3$) with $\mathrm{Re}(\gamma_j)>0$ are chosen by requiring a positive internal energy for the system to be in a steady state, as stated by Suo et al. [10].

The stress and electric displacement components can be expressed as follows

$$\sigma_{xz}^{*(n)}=-\sum_{j=1}^{3}\int_0^\infty \xi f_j\left[A_j^{(n)}(\xi,p)\cosh(\gamma_j\xi z)+B_j^{(n)}(\xi,p)\sinh(\gamma_j\xi z)\right]\sin(\xi x)d\xi \tag{11}$$

$$\sigma_{zz}^{*(n)}=P_0/p-\sum_{j=1}^{3}\int_0^\infty \xi g_j\left[A_j^{(n)}(\xi,p)\sinh(\gamma_j\xi z)+B_j^{(n)}(\xi,p)\cosh(\gamma_j\xi z)\right]\cos(\xi x)d\xi \tag{12}$$

$$\sigma_{xx}^{*(n)}=\sigma_0/p-\sum_{j=1}^{3}\int_0^\infty \xi q_j\left[A_j^{(n)}(\xi,p)\sinh(\gamma_j\xi z)+B_j^{(n)}(\xi,p)\cosh(\gamma_j\xi z)\right]\cos(\xi x)d\xi \tag{13}$$

$$D_z^{*(n)}=D_0/p-\sum_{j=1}^{3}\int_0^\infty \xi m_j\left[A_j^{(n)}(\xi,p)\sinh(\gamma_j\xi z)+B_j^{(n)}(\xi,p)\cosh(\gamma_j\xi z)\right]\cos(\xi x)d\xi \tag{14}$$

where $\sigma_0=C_{13}T_1+e_{31}T_2$ and the coefficients f_j, g_j, q_j, m_j are defined in Appendix A. By applying the boundary conditions (3) and (4), the unknown functions $B_j^{(1)}(\xi,p)$, $A_j^{(2)}(\xi,p)$, $B_j^{(2)}(\xi,p)$ ($j=1-3$) can be expressed by the independent unknowns $A_j^{(1)}(\xi,p)$ ($j=1-3$) as

$$\begin{aligned} &B_j^{(1)}(\xi,p)=\sum_{i=1}^{3}R_{ji}^{(1)}(\xi,h_1,p)A_i^{(1)}(\xi,p),\quad B_j^{(2)}(\xi,p)=\sum_{i=1}^{3}Q_{ji}(\xi,h_1,h_2,p)A_i^{(1)}(\xi,p) \\ &A_j^{(2)}(\xi,p)=\sum_{i=1}^{3}T_{ji}(\xi,h_1,h_2,p)A_i^{(1)}(\xi,p) \end{aligned} \tag{15}$$

where $R_{ji}^{(1)}(\xi,h_1,p)$, $T_{ji}(\xi,h_1,h_2,p)$ and $Q_{ji}(\xi,h_1,h_2,p)$ are known functions. Introduce the auxiliary functions $\Phi_i(x,p)$ ($i=1-3$) such that

$$\begin{Bmatrix}\Phi_1(x,p)\\ \Phi_2(x,p)\\ \Phi_3(x,p)\end{Bmatrix}=\frac{\partial}{\partial x}\begin{Bmatrix}u_x^{*(1)}(x,0^+,p)-u_x^{*(2)}(x,0^-,p)\\ u_z^{*(1)}(x,0^+,p)-u_z^{*(2)}(x,0^-,p)\\ \phi^{*(2)}(x,0^-,p)-\phi^{*(1)}(x,0^+,p)\end{Bmatrix} \tag{16}$$

By applying the solutions (7-9) and using the Fourier inverse transform, the independent unknowns can be obtained as

$$\begin{Bmatrix} A_1^{(1)}(\xi,p) \\ A_2^{(1)}(\xi,p) \\ A_3^{(1)}(\xi,p) \end{Bmatrix} = -\frac{2}{\pi\xi}\begin{bmatrix} Y_{11}(\xi,p) & Y_{12}(\xi,p) & Y_{13}(\xi,p) \\ Y_{21}(\xi,p) & Y_{22}(\xi,p) & Y_{23}(\xi,p) \\ Y_{31}(\xi,p) & Y_{32}(\xi,p) & Y_{33}(\xi,p) \end{bmatrix}\begin{Bmatrix} \int_0^c \Phi_1(s,p)\cos(s\xi)ds \\ \int_0^c \Phi_2(s,p)\sin(s\xi)ds \\ \int_0^c \Phi_3(s,p)\sin(s\xi)ds \end{Bmatrix} \tag{17}$$

where $Y_{ij}(\xi,p)$ $(i,j=1-3)$ are known functions. Satisfaction of the mixed boundary conditions (5) and (6) on the crack face plane leads to the simultaneous singular integral equations

$$\begin{aligned} &\int_{-1}^{1}\left\{\kappa_{m1}(s,x,p)\Psi_1(s,p)+\sum_{j=2}^{3}\left[\frac{U_{mj}^0}{s-x}+\kappa_{mj}(s,x,p)\right]\Psi_j(s,p)\right\}ds=\frac{-\pi T_m}{p} \\ &\int_{-1}^{1}\left\{\left[\frac{U_{31}^0}{x-s}+\kappa_{31}(s,x,p)\right]\Psi_1(s,p)+\sum_{j=2}^{3}\kappa_{3j}(s,x,p)\Psi_j(s,p)\right\}ds=0 \end{aligned} \qquad (m=1,2) \tag{18}$$

where $T_1=P_0$, $T_2=D_0$, $\Psi_i(s,p)=\Phi_i(cs,p)$, $\kappa_{ij}(s,x,p)$ $(i=1,2,3)$ are known kernel functions, the constants U_{ij}^0 are defined as $U_{ij}^0=\lim_{\xi\to\infty}U_{ij}(\xi,p)$ and $U_{ij}(\xi,p)$ are known functions. The functions $\Psi_i(s,p)$ $(i=1-3)$ satisfy the single-valuedness condition:

$$\int_{-1}^{1}\Psi_i(s,p)ds=0, \quad (i=1-3) \tag{19}$$

and $\Psi_i(s,p)$ may be expressed as

$$\Psi_i(s,p)=H_i(s,p)\Big/\sqrt{1-s^2} \tag{20}$$

where $H_i(s,p)$ $(i=1-3)$ are unknowns to be solved.

Use the Lobatto-Chebyshev method [11], singular integral equations (18) can be reduced to the following algebraic equations:

$$\sum_{i=1}^{n}A_i\left\{[\kappa_{m1}(x_k,s_i,p)]H_1(s_i,p)+\sum_{j=2}^{3}\left[\frac{U_{mj}^0}{s_i-x_k}+\kappa_{mj}(x_k,s_i,p)\right]H_j(s_i,p)\right\}=\frac{-\pi T_m}{p} \quad (m=1,2) \tag{21}$$

$$\sum_{i=1}^{n}A_i\left\{\left[\frac{U_{31}^0}{x_k-s_i}+\kappa_{31}(x_k,s_i,p)\right]H_1(s_i,p)+\sum_{j=2}^{3}[\kappa_{3j}(x_k,s_i,p)]H_j(s_i,p)\right\}=0 \tag{22}$$

$$\sum_{i=1}^{n}A_iH_j(s_i,p)=0 \qquad (j=1,2,3) \tag{23}$$

where,

$$s_i = \cos\left[\frac{(i-1)\pi}{n-1}\right], \quad (i=1,2,...,n); \quad x_k = \cos\left[\frac{(2k-1)\pi}{2(n-1)}\right], \quad (k=1,2,...,n-1)$$
$$A_i = \frac{\pi}{2(n-1)}, \quad (i=1,n); \quad A_i = \frac{\pi}{(n-1)}, \quad (i=2,3,...,n-1) \tag{24}$$

3. Asymptotic fields near the crack tip

Once functions $H_j(s,p)$ ($j=1,2,3$) are obtained from solving the algebraic equations (21-23), following the procedure in Li and Lee [12], the asymptotic expressions of the electro-elastic fields near the crack tip can be determined by introducing a polar coordinate system (r,θ) with the origin at the right crack tip, as follows

$$r = \sqrt{(x-c)^2 + z^2}, \quad \theta = \tan^{-1}\left[z/(x-c)\right] \tag{25}$$

The hoop and shear stresses at an angle θ near the right tip of the crack are obtained from the following relations in terms of the polar coordinates (r,θ)

$$\begin{aligned}\sigma^*_{\theta\theta}(r,\theta,p) &= \sigma^*_{zz}(r,\theta,p)\cos^2\theta + \sigma^*_{xx}(r,\theta,p)\sin^2\theta - \sigma^*_{xz}(r,\theta,p)\sin 2\theta \\ \sigma^*_{r\theta}(r,\theta,p) &= \sin 2\theta\left[\sigma^*_{zz}(r,\theta,p) - \sigma^*_{xx}(r,\theta,p)\right]/2 + \sigma^*_{xz}(r,\theta,p)\cos 2\theta\end{aligned} \tag{26}$$

Define the hoop stress intensity factor and shear stress intensity factor associated with the hoop and shear stresses at an arbitrary angle θ as [13]

$$K^*_{\theta\theta} = \lim_{r\to 0}\left(\sqrt{2r}\,\sigma^*_{\theta\theta}\right), \quad K^*_{r\theta} = \lim_{r\to 0}\left(\sqrt{2r}\,\sigma^*_{r\theta}\right) \tag{27}$$

Substituting Eqs. (26) into (27), the hoop and shear stress intensity factors in the Laplace domain can be obtained as:

$$K^*_{\theta\theta} = \sqrt{c}\sum_{j=1}^{3}\left\{\begin{aligned}&(g_j^0\cos^2\theta + q_j^0\sin^2\theta)\left[(-1)^n H_1(1,p)Y^0_{j1}\Lambda_{1j}(\theta) + \sum_{k=2}^{3} H_k(1,p)Y^0_{jk}\Lambda_{2j}(\theta)\right] \\ &- f_j^0\sin 2\theta\left[H_1(1,p)Y^0_{j1}\Lambda_{2j}(\theta) - (-1)^n\sum_{k=2}^{3} H_k(1,p)Y^0_{jk}\Lambda_{1j}(\theta)\right]\end{aligned}\right\} \tag{28}$$

$$K^*_{r\theta} = \sqrt{c}\sum_{j=1}^{3}\left\{\begin{aligned}&\frac{(g_j^0 - q_j^0)\sin 2\theta}{2}\left[(-1)^n H_1(1,p)Y^0_{j1}\Lambda_{1j}(\theta) + \sum_{k=2}^{3} H_k(1,p)Y^0_{jk}\Lambda_{2j}(\theta)\right] \\ &+ f_j^0\cos 2\theta\left[H_1(1,p)Y^0_{j1}\Lambda_{2j}(\theta) - (-1)^n\sum_{k=2}^{3} H_k(1,p)Y^0_{jk}\Lambda_{1j}(\theta)\right]\end{aligned}\right\} \tag{29}$$

where $0 \le \theta \le \pi$ when $n=1$ for the upper part and $-\pi \le \theta \le 0$ when $n=2$ for the lower part of the cracked layer, respectively; the angular functions $\Lambda_{1j}(\theta)$ and $\Lambda_{2j}(\theta)$ ($j=1,2,3$) are given in the following form

$$\Lambda_{nj}(\theta) = \sqrt{\frac{\sqrt{\cos^2(\theta) + \left[\gamma_j^0\sin(\theta)\right]^2} + (-1)^n\cos(\theta)}{2\left[\cos^2(\theta) + \left[\gamma_j^0\sin(\theta)\right]^2\right]}} \qquad (k=1,2) \tag{30}$$

in which the constants $g_j^0, q_j^0, f_j^0, Y_{ij}^0, \gamma_j^0$ are defined in Appendix A.

Note that by setting the angle θ equal to zero and using the relations in Eqs. (30), the common expressions for the Mode-I and Mode-II stress intensity factors can be obtained. The dynamic hoop and shear stress intensity factors can be obtained by performing the Laplace inverse transform to Eqs. (28) and (29) as

$$K_{\theta\theta}(\theta,t)=\frac{1}{2\pi i}\int_{Br}K_{\theta\theta}^{*}(\theta,p)\exp(pt)dp,\quad K_{r\theta}(\theta,t)=\frac{1}{2\pi i}\int_{Br}K_{r\theta}^{*}(\theta,p)\exp(pt)dp \tag{31}$$

where "Br" stands for the Bromwich path of integration. Different criteria have been proposed to predict the direction of crack branching [14]. Here we use the maximum hoop stress intensity factor criterion to predict crack kinking.

4. Numerical results and discussions

To study the effect of electro-elastic interaction on the stress field near the crack tip, the electric loading parameter $L_D=e_{33}D_0/(\lambda_{33}P_0)$ is introduced. The material constants of PCM-80 [15] are used in the following numerical calculation:

$$\begin{aligned}
&C_{11}=17.0\times10^{10}(\mathrm{N/m^2}),\ C_{13}=11.5\times10^{10}(\mathrm{N/m^2}),\ C_{33}=16.5\times10^{10}(\mathrm{N/m^2})\\
&C_{44}=3.05\times10^{10}(\mathrm{N/m^2}),\ e_{15}=13.7\ (\mathrm{C/m^2}),\ e_{31}=-5.99\ (\mathrm{C/m^2}),\\
&e_{33}=15.6\ (\mathrm{C/m^2}),\ \lambda_{11}=95.2\times10^{-10}(\mathrm{C^2/Nm^2}),\ \lambda_{33}=68.4\times10^{-10}(\mathrm{C^2/Nm^2})\\
&\rho=5.5\times10^{3}(\mathrm{Kg/m^3})
\end{aligned} \tag{32}$$

The variation of the normalized dynamic hoop stress intensity factors (HSIFs) $\frac{K_{\theta\theta}(t)}{P_0\sqrt{c}}$ with normalized time tV_s/c at different angles θ are displayed in Fig. 2. The shear wave velocity is defined as $V_s=\sqrt{c_{44}+\frac{e_{15}^2}{\lambda_{11}}\Big/\rho}$. Without loss of generality, the geometric size of the strip is taken to be $h_1/c=1,\ h_2/c=5$, and the applied electric loading parameter $L_D=+0.5$. Fig. 2 shows that the HSIFs increase as time increases, and reach their peak values at about $tV_s/c=3.5$, and then decrease and oscillate about their static values, until when $tV_s/c\to\infty$, HSIFs reduce to the static values. The peak values of the HSIF at $\theta=20$ degrees are bigger than that of $\theta=0$ degrees, which means that the crack tends to deviate from the original crack plane, provided that the material has the same fracture toughness in every direction.

Fig. 3 shows the variation of peak values of the dynamic hoop stress intensity factors versus angles θ when $L_D=+0.5$. For the case $h_1\neq h_2$, the maximum value of the HSIFs appears at an angle different from the original crack plane, which implies that the crack may kink in this particular direction. When $h_1/c=1,\ h_2/c=5$, the crack kinks at about $\theta=+20$ degrees, and in another case $h_1/c=5,\ h_2/c=1$, the crack kinks at about $\theta=-20$ degrees. It is evident that the

possible crack kinking direction is oriented toward the thinner side of the strip. This is in agreement with [16] and [8] for the static mixed mode crack problem. It also agrees with the physical phenomenon that surface cracking is more likely to happen, due to the mechanism the crack kinks into the direction toward the surface of the body. The maximum value of the HSIFs appear at the angle $\theta = 0$ in the symmetric case when $h_1 = h_2$, which implies that the crack may propagate along the extension of original crack plane.

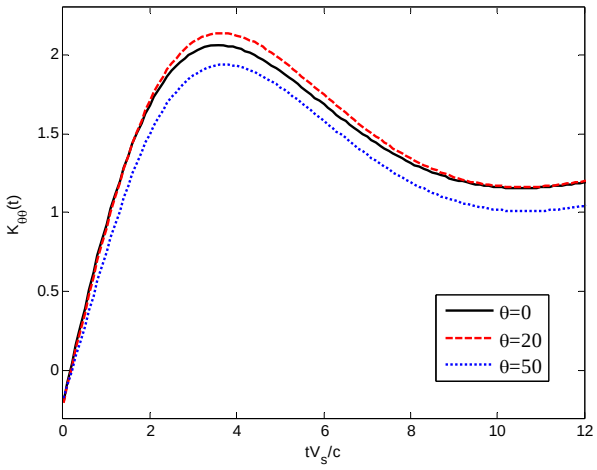

Figure 2. Dynamic hoop stress intensity factors for different angles

when $L_D = +0.5$, $h_1/c = 1$ and $h_2/c = 5$

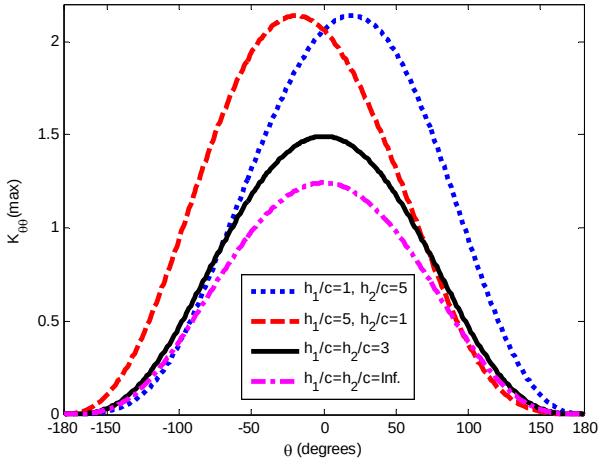

Figure 3. Maximum values of the normalized hoop stress intensity factors

versus angles when $L_D = +0.5$

Fig. 4 shows the effect of electric loading on the variation of normalized dynamic HSIFs at the angle $\theta = 20$ degrees. The electric loading parameter L_D affects the initial value and the peak value of the dynamic HSIFs. At the very beginning, a positive electric load leads to a lower initial value of the HSIF than negative electric load, whilst the peak value of the dynamic HSIFs induced by the positive electric load is higher than that for the negative electric load.

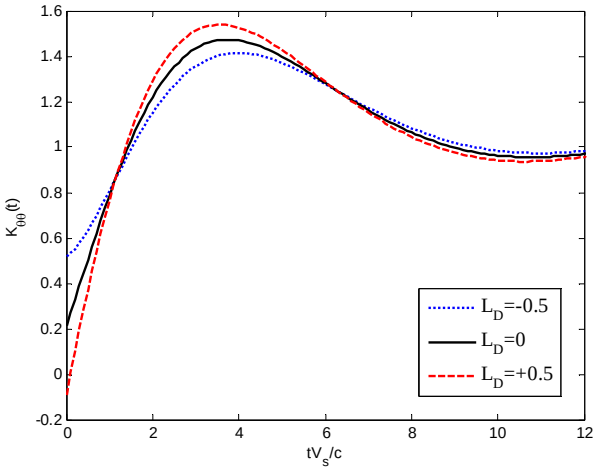

Figure 4. Dynamic hoop stress intensity factors for different electric loadings L_D

when $\theta = 20$ degrees and $h_2 = 2h_1 = 4c$

5. Concluding remarks

An impermeable crack in a piezoelectric strip under in-plane dynamic mechanical and electric loadings is studied. Fourier transforms are applied to reduce the mixed boundary value problem of the crack to dual integral equations, which are further expressed in terms of singular integral equations. Asymptotic fields near the crack tip are obtained in an explicit form and the corresponding field intensity factors are determined. The crack kinking phenomenon is investigated by applying the maximum hoop stress intensity factor criterion. Numerical results show that the geometry of the strip and the electric loading dominate the singular field distribution around the crack tip, and the hoop stress intensity factors are controlled by the material parameters, the electric loadings and the geometric size ratios.

Appendix A

The constants in Eqs. (14) and (15) are defined as

$$\mathrm{T}_1 = (\lambda_{33}P_0 + e_{33}D_0)/(C_{33}\lambda_{33} + e_{33}^2),\quad \mathrm{T}_2 = (e_{33}P_0 - C_{33}D_0)/(C_{33}\lambda_{33} + e_{33}^2) \tag{A.1}$$

$$\begin{Bmatrix} a_j \\ b_j \end{Bmatrix} = \begin{bmatrix} C_{11} + \rho p^2/\xi^2 - C_{44}\gamma_j^2 & e_{31} + e_{15} \\ (C_{13} + C_{44})\gamma_j^2 & e_{33}\gamma_j^2 - e_{15} \end{bmatrix}^{-1} \begin{Bmatrix} C_{13} + C_{44} \\ C_{33}\gamma_j^2 - C_{44} - \rho p^2/\xi^2 \end{Bmatrix} \tag{A.2}$$

$$f_j = C_{44}(a_j\gamma_j^2 + 1) - e_{15}b_j,\ \ g_j = (C_{13}a_j + e_{33}b_j - C_{33})\gamma_j$$
$$q_j = (C_{11}a_j + e_{31}b_j - C_{13})\gamma_j,\ \ m_j = (e_{31}a_j - \lambda_{33}b_j - e_{33})\gamma_j \tag{A.3}$$

$$g_j^0 = \lim_{\xi\to\infty} g_j,\ \ q_j^0 = \lim_{\xi\to\infty} q_j,\ \ f_j^0 = \lim_{\xi\to\infty} f_j,\ \ Y_{ij}^0 = \lim_{\xi\to\infty} Y_{ij}(\xi, p),\ \ \gamma_j^0 = \lim_{\xi\to\infty} \gamma_j(\xi, p) \tag{A.4}$$

References

[1] S.F. Li, P.A. Mataga, Dynamic crack propagation in piezoelectric materials-Part I: Electrode solution. J Mech Phys Solids, 44 (1996) 1799-1830.

[2] S.F. Li, P.A. Mataga, Dynamic crack propagation in piezoelectric materials-Part II: Vacuum solution. J Mech Phys Solids, 44 (1996) 1731-1866.

[3] Y. Shindo, H. Katsura, W. Yan, Dynamic stress intensity factor of a cracked dielectric medium in a uniform electric field. Acta Mech, 117 (1996) 1-10.

[4] Z.T. Chen, B.L. Karihaloo, S.W. Yu, A Griffith crack moving along the interface of two dissimilar piezoelectric materials, Int J Fract, 91(1998) 197-203.

[5] Z.T. Chen, S.W. Yu, Semi-infinite crack under anti-plane mechanical impact in piezoelectric materials. Int J Fract, 88 (1998) L53-56.

[6] X.Y. Wang, S.W. Yu, Transient response of a crack in piezoelectric strip subjected to the mechanical and electrical impacts: mode-I problem. Mech Mater, 33 (2001) 11-20.

[7] T. Zhu, W. Yang, Crack kinking in a piezoelectric solid. Int J Solids Struct, 36 (1999) 5013-5027.

[8] B.L. Wang, N. Noda, Mixed mode crack initiation in piezoelectric ceramic strip. Theor Appl Fract Mech, 34 (2000) 35-47.

[9] K.Q. Hu, Z. Zhong, A moving mode-III crack in a functionally graded piezoelectric strip. Int J Mech Mater Design, 2 (2005) 61-79.

[10] Z. Suo, C.-M. Kuo, D.M. Barnett, J.R. Willis, Fracture mechanics for piezoelectric ceramics. J Mech Phys Solids, 40 (1992) 739-765.

[11] P.S. Theocaris, N.I. Ioakimidis, Numerical integration methods for the solution of singular integral equations. Q Appl Math, 35 (1977) 173-183.

[12] X.F. Li, K.Y. Lee, Three-dimensional electroelastic analysis of a piezoelectric material with a penny-shaped dielectric crack. J Appl Mech, 71 (2004) 866-878.

[13] A. Azhdari, S. Nemat-Nasser, Hoop stress intensity factor and crack-kinking in anisotropic brittle solids. Int J Solids Struct, 33 (1996) 2023-2037.

[14] W. Yang, Mechatronic Reliability: Electric Failures, Mechanical-Electrical Coupling, Domain Switching, Mass-Flow Instabilities. Springer Verlag, New York, 2002.

[15] Y. Shindo, F. Narita, H. Mitsuru, Dynamic fatigue of cracked piezoelectric ceramics under electromechanical loading: Three-point bending test and finite element analysis. J Mech Mater Struct, 4 (2009) 719-729.

[16] J.W. Hutchinson, Z. Suo, Mixed mode cracking in layered materials. Adv Appl Mech, 29 (1992) 63-191.